

Electronic Supporting information

Second-coordination-sphere and electronic effects enhance iridium(III)-catalyzed homogeneous hydrogenation of carbon dioxide in water near ambient temperature and pressure

Wan-Hui Wang,^a Jonathan F. Hull,^b James T. Muckerman,^b Etsuko Fujita^{b,*}

and Yuichiro Himeda^{a,*}

^aNational Institute of Advanced Industrial Science and Technology,
Tsukuba Central 5-2, 1-1-1 Higashi, Tsukuba, Ibaraki 305-8565, Japan

^bChemistry Department, Brookhaven National Laboratory, Upton NY 11973, USA

*E-mail: himeda.y@aist.go.jp (Y. H.); fujita@bnl.gov (E.F.)

Experimental Section

Materials and Methods.

All manipulations were carried out under an argon atmosphere using standard Schlenk techniques or in a glovebox, and all aqueous solutions were degassed prior to use. ¹H NMR and ¹³C NMR spectra were recorded on Bruker Avance 400 and 500 spectrometers using tetramethylsilane or sodium 3-(trimethylsilyl)-1-propanesulfonate as an internal standard. pH values were measured on an Orion 3-Star pH meter with a glass electrode after calibration with standard buffer solutions. Elemental analyses were performed by a CE Instruments EA1110 elemental analyzer. Infrared spectra (KBr) were recorded on a FTIR spectrometer. UV-vis spectra were acquired using a JASCO V-550 UV/VIS spectrophotometer. Research grade CO₂ (>99.999%) and H₂ (>99.9999%), or mixed gas (CO₂/H₂ = 1/1) through O₂ trap was used for CO₂ hydrogenation; formate concentrations were monitored by an HPLC on an anion-exclusion column (Tosoh TSKgel SCX(H⁺)) using aqueous H₃PO₄ solution (20 mM) as eluent and a UV detector (λ = 210 nm). Water used in the reactions was obtained from a Simplicity water purification system. 6,6'-Dihydroxyl-2,2'-bipyridine¹ and 6,6'-dimethoxyl-2,2'-bipyridine (6,6'-(MeO)₂-bpy)² were synthesized according to the literature procedure. [Cp*Ir(H₂O)₃]SO₄, complexes **1** and **2** were prepared according to our previously reported procedures.³⁻⁵ All other chemicals were procured from commercial sources.

Synthesis of complexes 3a-c.

Synthesis of [Cp*Ir(6,6'-(OH)₂-bpy)(OH₂)]SO₄ (3a):**** 6DHBP (0.47 g, 2.5 mmol) was added to a 60 mL water solution of [Cp*Ir(H₂O)₃]SO₄ (1.19 g, 2.5 mmol) under argon atmosphere. After stirred at room temperature for 12 h, the solution was concentrated to about 5 mL and hold at 5 °C for 12 h. The precipitated solid was collected and dried under vacuum at 50 °C for 12 h to give 1.45 g yellow solid (yield: 92.1 %). ¹H NMR (500 MHz, D₂O): δ 8.01 (t, *J* = 10.0 Hz, 2H), 7.81 (d, *J* = 10.0, 2H), 7.20 (d, *J* = 10.0, 2H), 1.57 (s, 15H); ¹H NMR (500 MHz, D₂O/KOD): δ 7.97 (t, *J* = 8.0 Hz, 2H), 7.74 (d, *J* = 8.0 Hz, 2H), 7.13 (d, *J* = 8.0 Hz, 2H), 1.56 (s, 15H); ¹³C NMR (125 MHz, D₂O): δ 166.36, 156.62, 145.98, 117.80, 116.18, 91.30, 11.31; ¹³C NMR (125 MHz, D₂O/KOD): δ 172.01, 158.28, 140.80, 118.54, 108.68, 86.79, 11.35, 11.24. ESI-MS: calc. 515.1 [M-H₂O-H]⁺, found 515.2. Anal. Calc. for C₂₀H₂₅N₂O₇IrS·3H₂O: C 35.23, H 4.56, N 3.82.

Found: C 35.15, H 4.57, N 4.10.

[Cp*Ir(H)(6,6'-(O⁻)₂-bpy)]⁻: To the NMR tube, **3a** and KOD/D₂O solution (pH ~11) was added. The NMR tube was installed in a glass autoclave and charged with 0.5 MPa H₂. The NMR experiments were carried out after 3 h. ¹H NMR (500 MHz, D₂O/KOD): δ 7.38–7.35 (m, 2H), 6.95 (d, J = 10.0 Hz, 2H), 6.32 (d, J = 10.0 Hz, 2H), 1.54 (s, 15H), –10.56 (s, 1H); ¹³C NMR (125 MHz, D₂O/KOD): δ 173.21, 159.33, 139.51, 116.38, 108.76, 89.70, 11.98, 11.93. IR (KBr, cm⁻¹): 2041 (ν(Ir-H)).

[Cp*Ir(6,6'-(MeO)₂-bpy)(OH₂)]SO₄ (3b). ¹H NMR (500 MHz, D₂O): δ 8.26 (t, J = 8.0 Hz, 2H), 8.05 (d, J = 8.0 Hz, 2H), 7.45 (d, J = 8.0 Hz, 2H), 4.26 (s, 6H) 1.55 (s, 15H); ¹³C NMR (125 MHz, D₂O): δ 166.84, 156.93, 147.31, 119.48, 112.73, 91.67, 60.30, 11.18. ESI-MS: 543.3 [M-H₂O-H]⁺. Anal. Calc. for C₂₂H₂₉IrN₂O₇S·3H₂O: C 37.27, H 4.74, N 3.66. Found: C 37.12, H 4.96, N 3.94.

[Cp*Ir(6,6'-Me₂-bpy)(OH₂)]SO₄ (3c). ¹H NMR (500 MHz, D₂O): δ 8.29 (d, J = 8.0 Hz, 2H), 8.15 (t, J = 8.0 Hz, 2H), 7.83 (d, J = 8.0 Hz, 2H), 3.02 (s, 6H) 1.44 (s, 15H); ¹³C NMR (125 MHz, D₂O): δ 164.67, 158.79, 144.17, 131.15, 124.00, 91.74, 28.70, 10.73. ESI-MS: 511.3 [M-H₂O-H]⁺. Anal. Calc. for C₂₂H₂₉IrN₂O₇S·2.5H₂O: C 39.40, H 4.92, N 3.81. Found: C 39.39, H 5.11, N 4.01.

Procedure for catalytic hydrogenation of CO₂/bicarbonate at atmospheric conditions: A degassed aqueous NaHCO₃ or KHCO₃ solution (20 mL) of catalyst was vigorously stirred (1500 rpm) at atmospheric pressure of H₂/CO₂ (1:1) and room temperature. At appropriate intervals, samples were removed and analyzed by HPLC. The initial TOF was calculated from the initial rate, typically from the first 30 min.

Procedure for catalytic hydrogenation of CO₂/bicarbonate at pressurized conditions: A degassed aqueous NaHCO₃ or KHCO₃ solution (50 mL) of catalyst was stirred in a 100 mL stainless steel reactor equipped with a sampling device. The solution was stirred vigorously at the appropriate temperature under the desired pressure of CO₂/H₂ (1:1). Samples were

removed at appropriate intervals (typically 10, 30, 60, 90 and 120 min.) and analyzed by HPLC. The initial TOF was calculated from the initial part of the reaction (typically 10 min).

Hg poisoning experiment: A degassed 1 M NaHCO₃ solution (20 mL) of catalyst **3a** (1 µmol) was stirred in a 30 mL glass vessel equipped with a sampling device. The solution was stirred vigorously (1500 rpm) at 30 °C under 0.1 MPa of CO₂/H₂ (1:1). Samples were removed at appropriate intervals and analyzed by HPLC. 0.47 g Hg (2500 eq) was added at 90 min. The plot of turnovers vs reaction time was shown in Figure S4.

Theoretical methods

All calculations were carried out using the Gaussian09⁶ suite of programs with density functional theory using the B3LYP functional⁷ with the cep-121g basis⁸ for Ir and the 6-31+G(d,p) basis⁹ for all other elements. Molecular geometry was optimized and vibrational frequencies were calculated in the gas phase. A single-point calculation using the 6-311++G(d,p) basis¹⁰ and the CPCM continuum solvation model¹¹ with UAHF radii was then performed to obtain the sum of an improved electronic energy and the solvation free energy.

A free-energy profile along the postulated sequence of intermediates for CO₂ hydrogenation was obtained as the sum of the system (i.e., catalyst species) and reservoir (i.e., reactants or products apart from the catalyst complex) free energies. The free-energy profile was adjusted to the non-standard state conditions of pH 8.3 instead of pH 0 through the use of the equation

$$\Delta G = RT \ln \left(\frac{Q}{K_{eq}} \right),$$
 where Q is the same ratio of species concentrations as K_{eq} except that the

concentration values are arbitrary. At equilibrium, when $Q = K_{eq}$, $\Delta G = 0$, and when $Q = 1$ (i.e., standard state conditions) $\Delta G = \Delta G^* = -RT \ln(K_{eq})$. In the present case, all species remain in their standard states except H⁺, for which [H⁺] is taken to be 10^{-pH} M. This correction for pH affects only those steps in which a proton is involved (see Table S2 and Fig. S6).

An intrinsic reaction coordinate (IRC) calculation was carried out the heterolysis of H₂ in the gas phase to determine whether or not the pendent base –O[–] species were involved in the reaction. These calculations were performed without vibrational frequency calculations, hence the energetics along the resulting pathway only reflect the electronic energy contribution, and not the zero-point energy changes or the significant entropic contribution. This IRC is shown in Fig. S7.

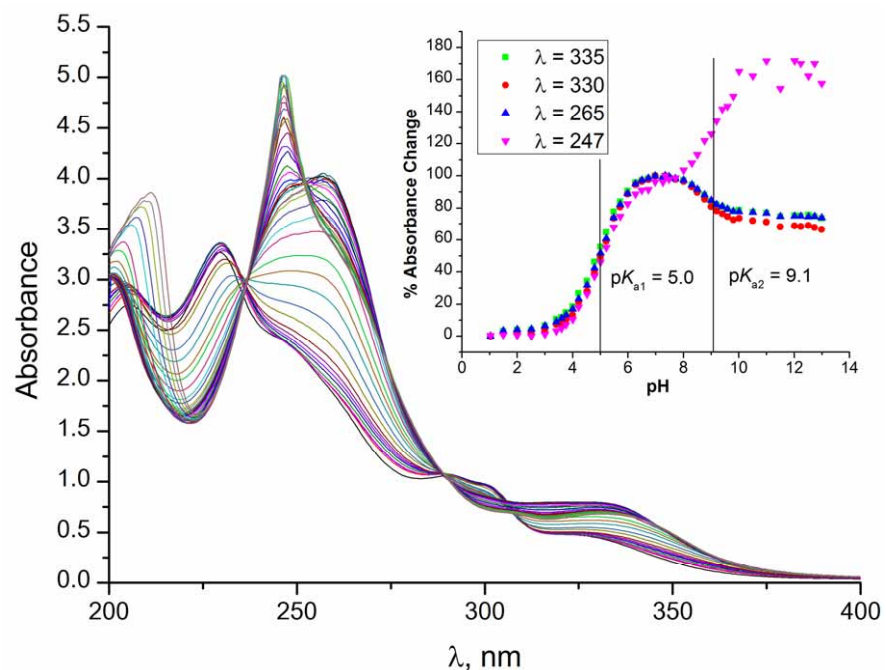


Figure S1. UV-pH titration with **1a**.³ Inset shows single wavelength data and Boltzmann fits used to determine the pK_a values of the ligand hydroxyl groups, and the H_2O ligand.

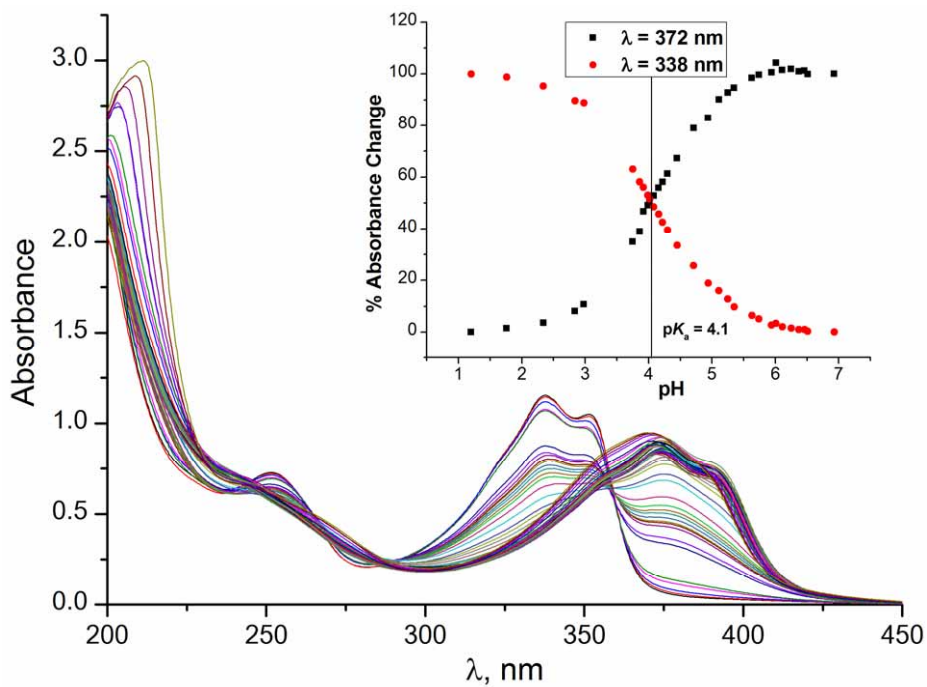


Figure S2. UV-pH titration with **3a**. Inset shows single wavelength data and Boltzmann fits used to determine the pK_a values of the ligand hydroxyl groups.

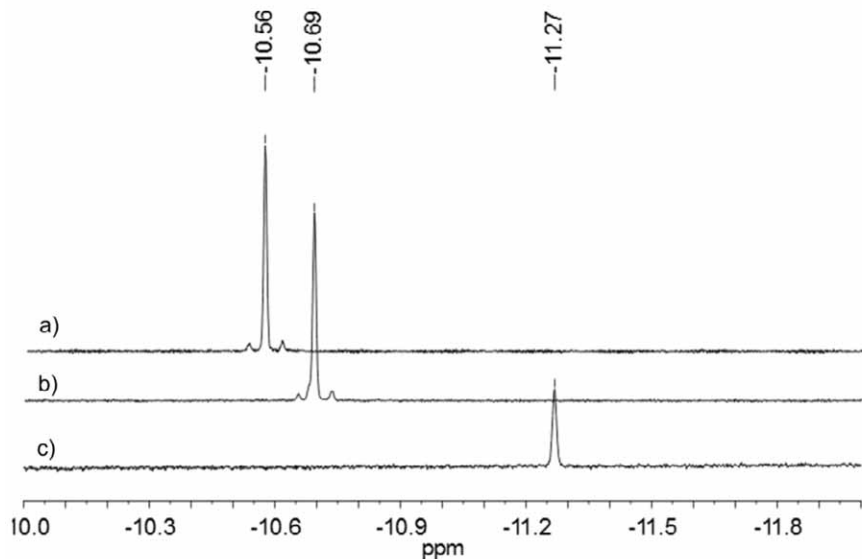


Figure S3. Partial ¹H NMR spectra of Ir-hydride synthesized from a) **3a**, b) **2**, c) **1a**.

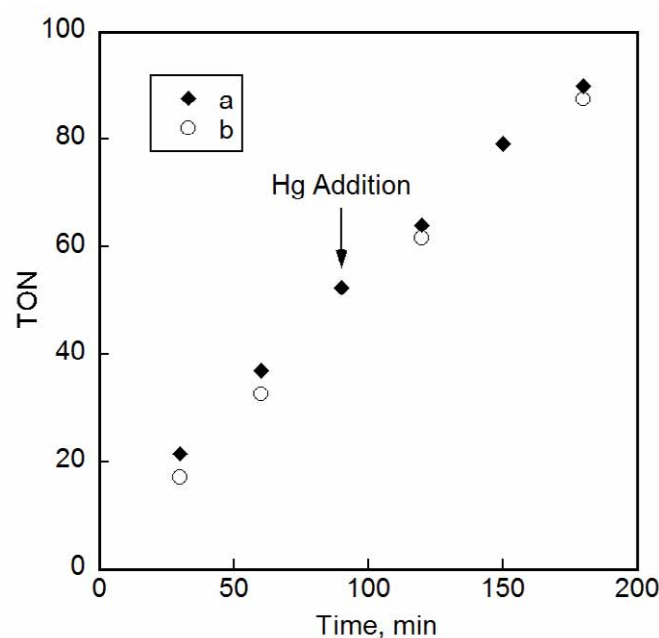


Figure S4. The plot of turnovers vs reaction time for the mercury test in the hydrogenation of CO₂. Reaction conditions: catalyst **3a** (1 μ mol), 1 M NaHCO₃ solution, 30 °C, 0.1 MPa of CO₂/H₂ (1:1); a) 0.47 g (2500 eq) Hg was added at 90 min; b) without Hg.

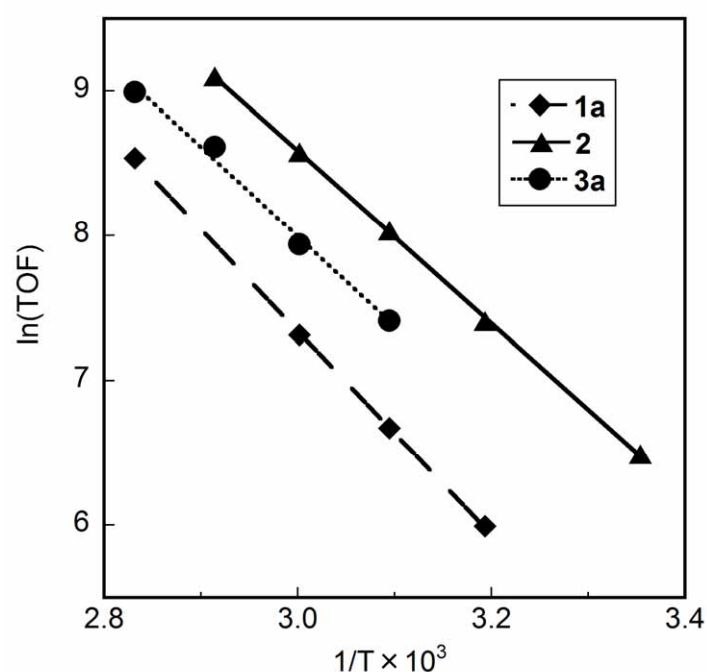


Figure S5. Arrhenius plots of initial rates for hydrogenation of CO₂ using **1a**, **2**, and **3a** in 1 M NaHCO₃ under 1 MPa H₂/CO₂ (1/1). From this figure, the activation energies for **1a**, **2**, and **3a** are calculated to be 58.5, 49.5, and 51.4 kJ mol⁻¹ respectively.

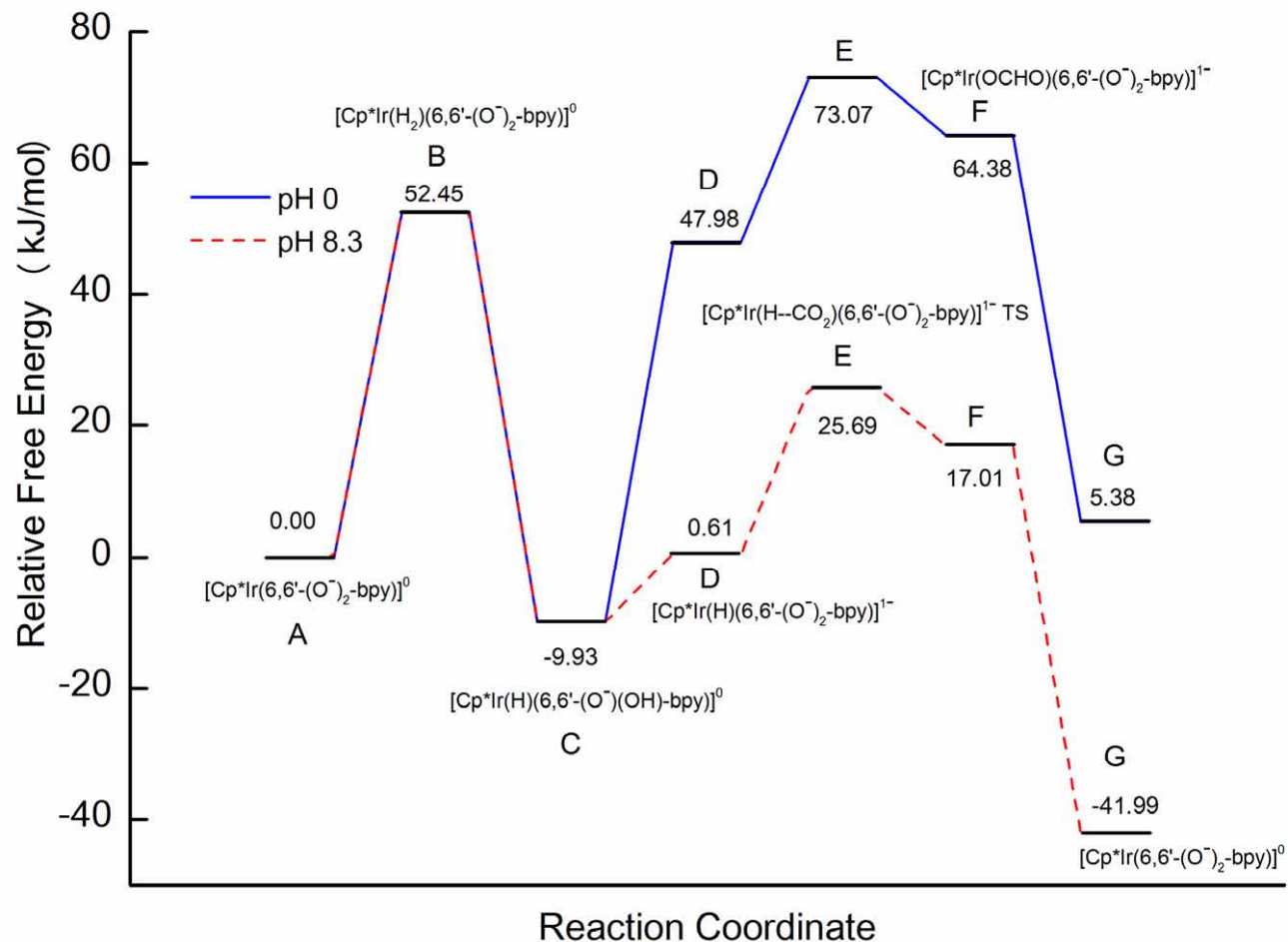


Figure S6. Calculated free-energy profiles for the proposed catalytic cycle of **3a** for conversion of H₂ and CO₂ into H⁺ and formate at pH 8.3 and formic acid at pH 0. The transition state for CO₂ insertion into the Ir—H bond is very “late”, almost at the geometry of the formate complex, however, the transition state has an imaginary frequency of 134*i* cm⁻¹, while the formate complex has all real frequencies. The two species differ in free energy by only ca. 8.7 kJ mol⁻¹.

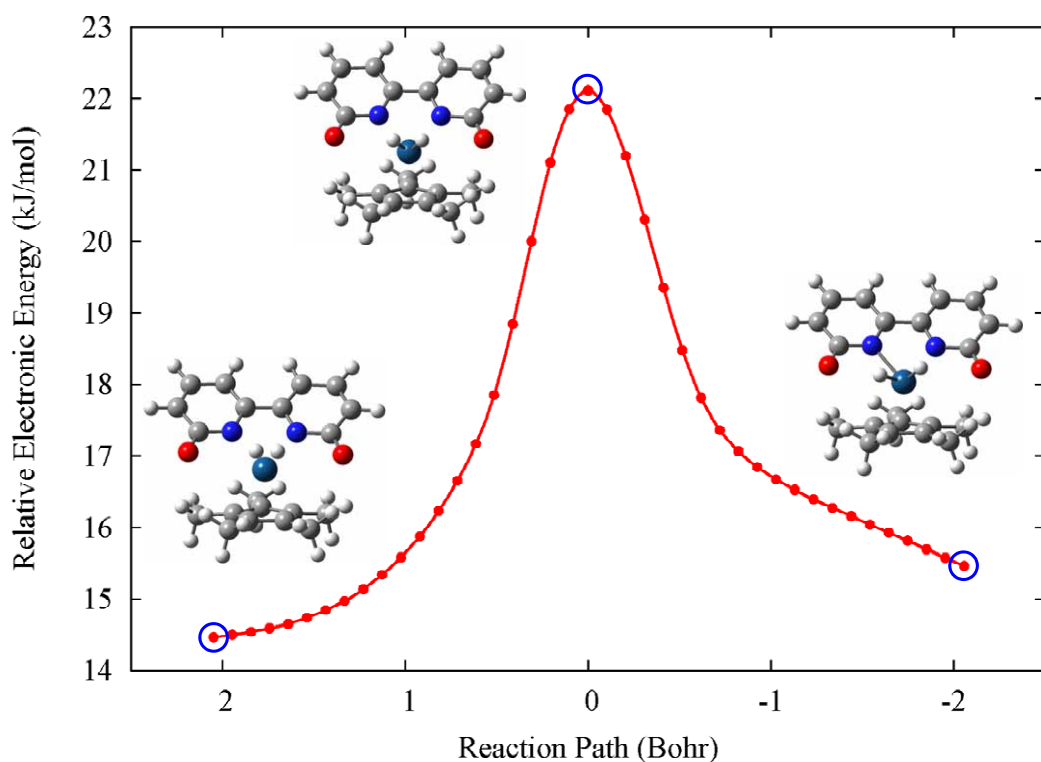


Figure S7. Calculated intrinsic reaction coordinate (IRC) for H_2 heterolysis by **3a**. The electronic energy along this pathway is relative to that of $[\text{Cp}^*\text{Ir}(6,6'-(\text{O}^-)_2\text{-bpy})]^0$ in solution plus that of H_2 in the gas phase. The electronic energy of the transition state (22.1 kJ mol^{-1}) is much smaller than the corresponding standard free energy of activation (52.4 kJ mol^{-1}) owing to a large entropic effect.

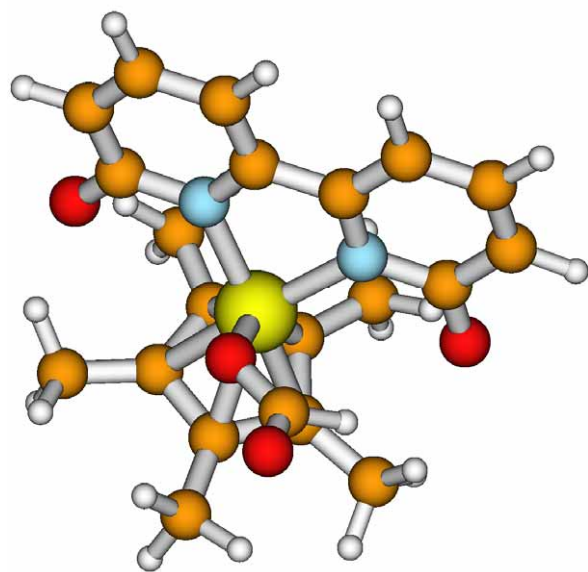


Figure S8. Optimized structure of species **E** in which CO₂ insertion is stabilized by a weak hydrogen bonding interaction (3.127 Å) with the deprotonated pendent base.

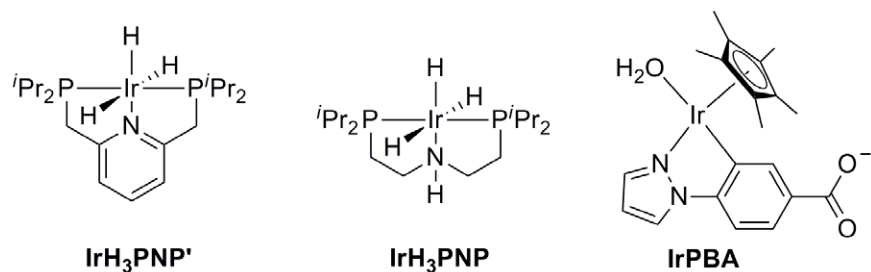


Figure S9. Structure of the complexes involved in Table 1.

Table S1. Initial rates and rate differences of catalysts **1** and **3** for hydrogenation of CO₂.^a

	1		3	
R	Initial TOF / h ⁻¹	Log(k_R/k_H)	Initial TOF / h ⁻¹	Log(k_R/k_H)
H	4.7	0	3.5	0
Me	12	0.41	30	0.94
MeO	49	1.02	565	2.21
O ⁻	5100	3.04	8050	3.36

^a Reaction conditions: 1) [Cp*Ir(4,4'-(R)₂-bpy)(OH₂)]SO₄ **1** (0.02-0.2 mM) in 1 M KOH at 80 °C under 1 MPa of H₂/CO₂ (1/1). 2) [Cp*Ir(6,6'-(R)₂-bpy)(OH₂)]SO₄ **3** (0.01-0.2 mM) in 1 M NaHCO₃ at 80 °C under 1 MPa of H₂/CO₂ (1/1).

Table S2. Calculated energetics of system plus reservoir for the postulated catalytic cycle of complex **3a**. Relative energies are with respect to $\text{Cp}^*\text{Ir}(6,6'\text{-ObpyO})^0$ ^a (**A**) in 1 M solution, $\text{H}_{2(\text{g})}$ and $\text{CO}_{2(\text{g})}$ at 1 atm partial pressure, and $\text{H}_2\text{O}_{(\text{liq})}$ as a pure liquid.

Species	$E_{\text{el(g)}}^{\text{a}}$ (Hartree)	$G_{(\text{g})}^{\text{o}}{}^{\text{a}}$ (Hartree)	$E_{\text{el(g)}} + \Delta G_{\text{s}}^*$ ^b (Hartree)	G_{s}^* ^c (Hartree)	Reservoir Species	Reservoir G^* (Hartree)	System + Res. G^* (Hartree)	Rel. ΔG^* (kJ/mol)	Rel. ΔG @ pH 8.3 (kJ/mol)
$[\text{Cp}^*\text{Ir}(6,6'\text{-}(\text{O}^-)_2\text{-bpy})\text{(OH}_2\text{)}]^0 \text{A}^*$	-1216.158361	-1215.820541	-1216.453228	-1216.112389	$\text{H}_{2(\text{g})}, \text{CO}_{2(\text{g})}$	-189.776905	-1405.939919	34.8250	34.8250
$[\text{Cp}^*\text{Ir}(6,6'\text{-}(\text{O}^-)_2\text{-bpy})]^0 \text{A}$	-1139.713117	-1139.398878	-1139.977353	-1139.660095	$\text{H}_{2(\text{g})}, \text{CO}_{2(\text{g})}, \text{H}_2\text{O}_{(\text{liq})}$	-266.214468	-1405.953183	0.0000	0.0000
$[\text{Cp}^*\text{Ir}(\text{H}_2)(6,6'\text{-}(\text{O}^-)_2\text{-bpy})]^0 \text{TS B}$	-1140.883669	-1140.556909	-1141.150832	-1140.821054	$\text{CO}_{2(\text{g})}, \text{H}_2\text{O}_{(\text{liq})}$	-265.112152	-1405.933205	52.4519	52.4519
$[\text{Cp}^*\text{Ir}(\text{H})(6,6'\text{-}(\text{HO})(\text{O}^-)\text{-bpy})]^0 \text{C}$	-1140.902155	-1140.568665	-1141.181320	-1140.844812	$\text{CO}_{2(\text{g})}, \text{H}_2\text{O}_{(\text{liq})}$	-265.112152	-1405.956964	-9.9263	-9.9263
$[\text{Cp}^*\text{Ir}(\text{H})(6,6'\text{-}(\text{O}^-)_2\text{-bpy})]^- \text{D}$	-1140.386248	-1140.067443	-1140.710841	-1140.389017	$\text{H}^+_{(\text{s})}, \text{CO}_{2(\text{g})}, \text{H}_2\text{O}_{(\text{liq})}$	-265.545890	-1405.934908	47.9828	0.6063
$[\text{Cp}^*\text{Ir}(\text{H})(\text{CO}_2)(6,6'\text{-}(\text{O}^-)_2\text{-bpy})]^- \text{TS E}$	-1328.974989	-1328.642779	-1329.361282	-1329.026054	$\text{H}^+_{(\text{s})}, \text{H}_2\text{O}_{(\text{liq})}$	-76.899297	-1405.925351	73.0739	25.6974
$[\text{Cp}^*\text{Ir}(\text{HCO}_2)(6,6'\text{-}(\text{O}^-)_2\text{-bpy})]^- \text{F}$	-1328.976354	-1328.645613	-1329.363123	-1329.029364	$\text{H}^+_{(\text{s})}, \text{H}_2\text{O}_{(\text{liq})}$	-76.899297	-1405.928661	64.3829	17.0064
$[\text{Cp}^*\text{Ir}(6,6'\text{-}(\text{O}^-)_2\text{-bpy})]^0 \text{G}$	-1139.713117	-1139.398878	-1139.977353	-1139.660095	$\text{H}^+_{(\text{s})}, \text{HCO}_2^-_{(\text{s})}, \text{H}_2\text{O}_{(\text{liq})}$	-266.291037	-1405.951132	5.3858	-41.9908

^a B3LYP/cep-121g; 6-31++G(d,p) in the gas phase.

^b B3LYP/cep-121g; 6-311++G(d,p) with CPCM treatment of water solvent using UAHF radii.

^c $(E_{\text{el(g)}} + \Delta G_{\text{s}}^*) + G_{(\text{g})}^{\text{o}} - E_{\text{el(g)}} + \Delta G^{\text{o} \rightarrow *}$.

References

- [1] Umemoto, T.; Nagayoshi, M.; Adachi, K.; Tomizawa, G. *J. Org. Chem.* **1998**, *63*, 3379.
- [2] Manandhar, S.; Singh, R. P.; Eggers, G. V.; Shreeve, J. n. M. *J. Org. Chem.* **2002**, *67*, 6415.
- [3] Himeda, Y.; Onozawa-Komatsuzaki, N.; Miyazawa, S.; Sugihara, H.; Hirose, T.; Kasuga, K. *Chem.-Eur. J.* **2008**, *14*, 11076.
- [4] Himeda, Y. *Green Chem.* **2009**, *11*, 2018.
- [5] Hull, J. F.; Himeda, Y.; Wang, W.-H.; Hashiguchi, B.; Periana, R.; Szalda, D. J.; Muckerman, J. T.; Fujita, E. *Nat. Chem.* **2012**, *4*, 383.
- [6] Gaussian 09, Revision B.01, M. J. Frisch, G. W. Trucks, H. B. Schlegel, G. E. Scuseria, M. A. Robb, J. R. Cheeseman, G. Scalmani, V. Barone, B. Mennucci, G. A. Petersson, H. Nakatsuji, M. Caricato, X. Li, H. P. Hratchian, A. F. Izmaylov, J. Bloino, G. Zheng, J. L. Sonnenberg, M. Hada, M. Ehara, K. Toyota, R. Fukuda, J. Hasegawa, M. Ishida, T. Nakajima, Y. Honda, O. Kitao, H. Nakai, T. Vreven, J. A. Montgomery, Jr., J. E. Peralta, F. Ogliaro, M. Bearpark, J. J. Heyd, E. Brothers, K. N. Kudin, V. N. Staroverov, R. Kobayashi, J. Normand, K. Raghavachari, A. Rendell, J. C. Burant, S. S. Iyengar, J. Tomasi, M. Cossi, N. Rega, J. M. Millam, M. Klene, J. E. Knox, J. B. Cross, V. Bakken, C. Adamo, J. Jaramillo, R. Gomperts, R. E. Stratmann, O. Yazyev, A. J. Austin, R. Cammi, C. Pomelli, J. W. Ochterski, R. L. Martin, K. Morokuma, V. G. Zakrzewski, G. A. Voth, P. Salvador, J. J. Dannenberg, S. Dapprich, A. D. Daniels, O. Farkas, J. B. Foresman, J. V. Ortiz, J. Cioslowski, and D. J. Fox, Gaussian, Inc., Wallingford CT, 2009.
- [7] (a) Becke, A. D. *Phys. Rev. A* **1988**, *38*, 3098; (b) Lee, C.; Yang, W.; Parr, R. G. *Phys. Rev. B* **1988**, *37*, 785; (c) Vosko, S. H.; Wilk, L.; Nusair, M. *Can. J. Phys.* **1980**, *58*, 1200; (d) Becke, A. D. *J. Chem. Phys.* **1993**, *98*, 5648; (e) Stephens, P. J.; Devlin, F. J.; Chabalowski, C. F.; Frisch, M. J. *J. Phys. Chem.* **1994**, *98*, 11623.
- [8] Stevens W. J.; Krauss M.; Basch H.; and Jasien P. G., *Can. J. Chem.* **1992**, *70*, 612-30.
- [9] Hehre W.J.; Ditchfield R.; and Pople J. A., *J. Chem. Phys.* **1972**, *56*, 2257.
- [10] Ditchfield R.; Hehre W. J.; and Pople J. A., *J. Chem. Phys.* **1971**, *54*, 724.
- [11] (a) Barone V.; Cossi, M. *J. Phys. Chem. A* **1998**, *102*, 1995; (b) Cossi, M.; Rega, N.; Scalmani, G.; Barone, V. *J. Comp. Chem.* **2003**, *24*, 669; (c) Klamt, A.; Schuurmann, G. *J. J. Chem. Soc., Perkin Trans.* **1993**, *2*, 799.